Thermal and DMA Characterization of PTFE-PMMA Nanocomposites from Core-Shell Nanoparticles

Diego Antonioli,[1] *Michele Laus,*[*1] *Katia Sparnacci,*[1] *Simone Deregibus,*[1] *Valerj Kapeliouchko,*[2] *Giovanna Palamone,*[2] *Tiziana Poggio,*[2] *Giampaolo Zuccheri,*[3] *Rosita Passeri*[3]

Summary: The thermal and dynamic-mechanical characteristics of three PTFE/PMMA nanoparticle samples are described. The shell forming PMMA, once isolated from the PTFE cores, exhibits a lower thermal stability than the PMMA component in the corresponding nanocomposite under both thermal and oxidative degradation conditions thus indicating a definite, though moderate, thermal reinforcement due to the morphology of the nanocomposites. An increase in the thermal stability under nitrogen atmosphere was observed as the PTFE amount increases. However under air, no difference is observed in the various systems. These observations suggest that only a physical shield can be exerted by the PTFE cores to the PMMA matrix possibly due to a weak interface between PTFE and the PMMA. This hypothesis is also substantiated by the DMA analysis.

Keywords: core-shell nanoparticles; DMA; PMMA; PTFE; TGA

Introduction

A mild and extremely efficient strategy to produce compounds featuring a perfect distribution of PTFE particles within the polymer matrix is based on the preparation of core-shell particles in which the core is constituted by PTFE and the shell by the technopolymer of interest. A perfect dispersion of the PTFE nanoparticles is obtained when the matrix is constituted by the same polymer with which the shell is made up. We have recently employed this approach to prepare PTFE/PS[1] and PTFE/PMMA[2,3] nanoparticles using PTFE latexes, with particles in the submicrometer range, as seeds in the emulsifier-free emulsion polymerization of the corresponding monomers. In general, no residual PTFE or secondary nucleation was observed. The particle size is dictated by the ratio between the monomer and the PTFE seed in the reaction mixture. In addition, the particle size distribution was always quite narrow. Accordingly, the above core-shell nanoparticles represent a novel class of highly specific but very efficient PTFE-based additives capable of being perfectly dispersed into PS, PMMA and miscible polymer matrices as well.

In addition, the possibility of controlling the particle size, while still keeping the particle size distribution narrow, could be of particular relevance in the view of the final use of these systems as building blocks for nanocomposites, including photonic crystals, with tuneable periodicities.

The present paper focuses on the thermal and dynamic-mechanical characteristics of three PTFE/PMMA core-shell nanoparticle samples. In particular, the thermal and oxidative degradation of the

[1] Dipartimento di Scienze dell' Ambiente e della Vita and UdR Alessandria INSTM, Università del Piemonte Orientale, 15100 Alessandria, Italy
Fax(+39)0131 360250; E-mail: laus@mfn.unipmn.it
[2] Solvay Solexis SpA, Spinetta Marengo, 15100 Alessandria, Italy
[3] Dipartimento di Biochimica "G. Moruzzi", S3 center of the National Institute for the Physics of the Matter (CNR) and UdR Bologna INSTM, Università di Bologna, 40126 Bologna, Italy

PMMA component of the particles was studied by thermogravimetry and the results compared with the shell-forming PMMA alone once isolated from the corresponding nanoparticle samples. Definite, though moderate, thermal and mechanical reinforcement is observed assigned to the peculiar nanostructured morphology.

Experimental Part

Materials

PTFE latex DV2 was provided by Solvay Solexis and consists of particles with spherical shape, average diameter of 33 nm and narrow size distribution. The preparation of samples DV2M1, DV2M4 and DV2M6 was previously reported.[3] The characteristics of these samples are collected in Table 1.

Characterization

SFM analysis was performed with Tapping-Mode Atomic Force Microscopy in air on a Multimode Nanoscope IIIa instrument (Veeco, S. Barbara, CA, U.S.A.) operated in constant amplitude mode. Scanning electron microscope (SEM) images were obtained using a Zeiss Gemini 1530 SEM. The sample was sputter coated under vacuum with a thin layer (10–30 Å) of gold. Thermogravimetric analysis (TGA) was performed using a Mettler thermobalance at a scanning rate of 10 °C/min from room temperature up to 800 °C under air or nitrogen flow. Differential scanning calorimetry (DSC) was carried out using a Mettler-Toledo DSC 821 apparatus. Samples of about 5 mg were employed. The instrument was calibrated with high purity standards. Dry nitrogen was used as purge gas. The PMMA shell forming material was isolated by adding 1.0 ml of THF to about 100 mg of the core-shell sample. After centrifugation at 18000 rpm for 20 min, quantitative sedimentation of the PTFE was obtained. Then supernatant was withdrawn and the solvent evaporated under reduced pressure. The samples for the dynamic-mechanical analysis were prepared introducing the powder sample into a rectangular mould. The entire assembly was then placed between press plates with a nominal pressure of 4.9×10^7 Pa and allowed to stand at room temperature for 20 min. The temperature was then raised to 160 °C and the pressure released to 4.9×10^6 Pa. After 15 min, the sample was quenched into cold water and recovered as rectangular $20 \times 5 \times 2$ mm sheets. The modulus was measured with a dynamic mechanical analyzer Rheometric DMTA V, employing the single cantilever flexural geometry. A scanning rate of 4 °C/min was chosen.

Results and Discussion

The PTFE/PMMA core-shell nanoparticles were prepared, as previously described,[3] by emulsifier-free seeded methylmethacrylate emulsion polymerization using a PTFE latex, marked DV2, consisting of spherical particles with average diameters of 33 nm, as the seed. Several core-shell samples were prepared with different size and composition. For the present study, three samples marked DV2M1, DV2M4 and DV2M6 were employed. Their size and composition data are collected in Table 1 whereas Figure 1 reports the SEM and SFM images of sample DV2M4, as a typical example.

Table 1.
Size, composition, molecular weight data of the various samples.

Sample	d PCS (nm)	d SEM ± SD (nm)	% PTFE theorical (W/W)	%PTFE (DSC)	%PTFE (TGA)
DV2M1	96.2	69 ± 8	5.5	5.3	5.5
DV2M4	72.7	54 ± 6	14.9	15.1	14.8
DV2M6	62.9	48 ± 8	25.9	25.8	20.3

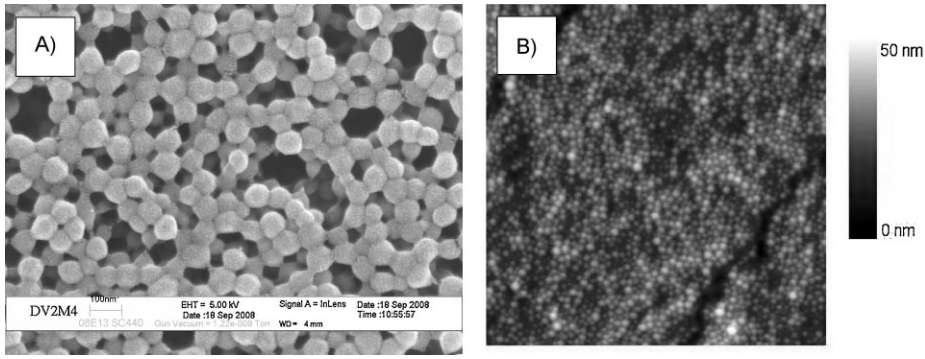

Figure 1.
A. SEM micrograph of sample DV2M4. B. Tapping-mode AFM images of the DV2M4 specimen showing a narrow distribution of particle diameters and some local ordering in the cast multilayer film. Image size is 3 μm, the nanoparticle heights are coded in shades of color according to the attached look-up table.

The thermal behavior of the various samples was studied by combined differential scanning calorimetry and thermogravimetric analysis. The melting of DV2, with a heating rate of 10 °C/min, occurs at 326 °C (Figure 2e) and the minimum of the crystallization exotherm, with a cooling rate of −10 °C/min, is observed at 310 °C (Figure 2a), in agreement with literature data. The melting of the PTFE cores in samples DV2M1, DV2M4 and DV2M6 at 10 °C/min is also observed at 326 °C whereas single crystallization exotherms are observed with minimum at 260°C, on cooling at −20 °C/min, after a fast heating (200 °C/min) to 330 °C. Fast heating is necessary to avoid or at least reduce the PMMA degradation, as discussed in detail in ref. 4.

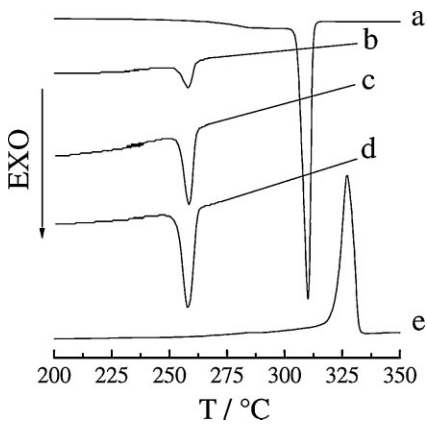

Figure 2.
DSC first cooling (a) and second heating (e) at 10 °C/min of DV2 sample. DSC cooling traces after fast heating (200 °C/min) to 330 °C at 20 °C/min of DV2M1 (b), DV2M4 (c) and DV2M6 (d) samples.

The single crystallization process at very high undercooling derives from the homogeneous nucleation of the PTFE core within the PMMA matrix. This behavior[4] indicates that, in the present samples, the PTFE cores are completely surrounded by PMMA.

The thermal stability of samples DV2M1, DV2M4 and DV2M6 was investigated by thermogravimetric analysis. Figure 3 reports the TGA curves, also represented in the derivative form (DTG), of sample DV2M1 under nitrogen and air atmosphere. The weight losses observed at 100–400 °C and at 500 °C are assignable to PMMA and PTFE decomposition, respectively. Under nitrogen atmosphere and in the 100–400 °C range, there is a succession of losses typical for radically polymerized PMMA[5] and are attributed to reactions including the chain scission at the head-head linkages (170 °C), the chain end initiation from vinylidene chain ends (270 °C) and the random scission initiation within the polymer chains (370 °C). Under air atmosphere, the degradation processes caused by the weak linkages at low

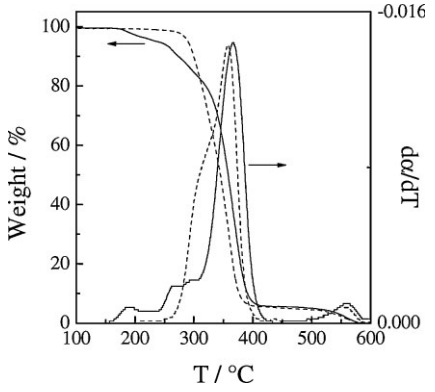

Figure 3.
TGA and DTG curves of DV2M1 core – shell sample at 10 °C/min degraded in nitrogen (solid line) and air (dash line).

temperature are suppressed, or at least inhibited, through a radical trapping reaction provided by the oxygen whereas the degradation at high temperature is enhanced.

Figure 4 reports the TGA curves of sample DV2M6 under nitrogen and air as well as the TGA curves of the shell-forming PMMA of the same sample. The shell-forming PMMA was separated from PTFE through addition of THF to the core-shell sample and centrifugation at 18000 rpm. In these conditions, quantitative sedimentation of PTFE was obtained and the PMMA was recovered from the supernatant. The pure PMMA material exhibits a lower thermal stability than the corresponding PMMA component in the presence of the PTFE under both thermal and oxidative degradation conditions.

A similar effect is observed also for the other samples and indicates a definite though moderate thermal reinforcement due to the morphology of the nanocomposites.

Figures 5 and 6 illustrate collectively the TGA curves for the three samples. Under nitrogen, it is quite evident that the thermal degradation curve is shifted toward higher values along the temperature scale as the PTFE amount increases. In addition, the lower temperature degradation processes caused by the weak linkages are suppressed, or at least inhibited. A similar enhanced thermal resistance was described in other nanostructured systems including exfoliated layered hydroxides/PMMA[6] and silica[7] or clay/PMMA[8] nanocomposites. This effect was tentatively explained by the trapping effect of the dispersed phase on the decomposition products. Alternatively, the enhanced thermal resistance was ascribed to the prevention of out

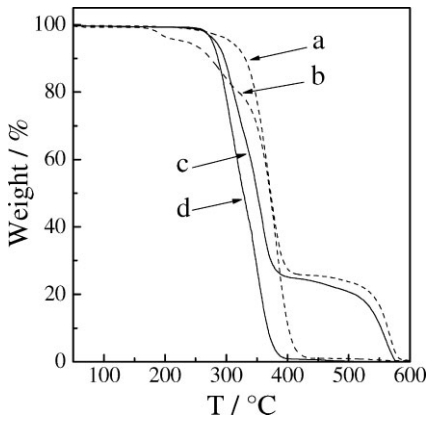

Figure 4.
TGA curves at 10 °C/min for DV2M6 sample under nitrogen (dashed line) and air (continuous line): core-shell under nitrogen (a), shell under nitrogen (b), core-shell under air (c) and shell under air (d).

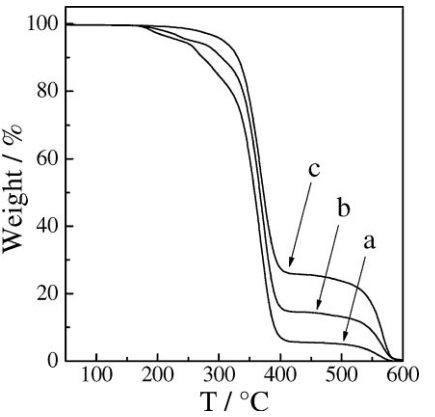

Figure 5.
TGA curves for three samples of core-shell nanoparticles at 10 °C/min under nitrogen: DV2M1 (a), DV2M4 (b) and DV2M6 (c).

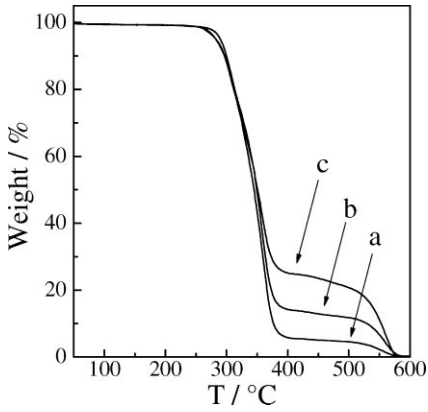

Figure 6.
TGA curves for three samples of core-shell nanoparticles at 10 °C/min under air: DV2M1 (a), DV2M4 (b) and DV2M6 (c).

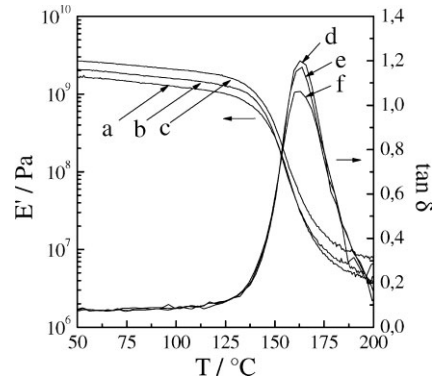

Figure 7.
Trend of the storage modulus E′ and loss tangent tan δ as a function of temperature. Storage modulus E′: DV2M1 (a), DV2M4 (b) and DV2M6 (c). Loss tangent tan δ: DV2M1 (d), DV2M4 (e) and DV2M6 (f).

diffusion of the volatile gasses from the thermally decomposed products because the dispersed phase acts as gas barrier reducing the gas permeability. In the present system, this last hypothesis appears more reasonable than the former because the C-F bond is too strong to allow radical trapping through fluorine transfer reactions. Quite surprisingly, under air, no difference is observed in the various systems.

It is pertinent to note that compounds produced by a reactive extrusion process[9,10] between electron-beam-irradiated PTFE and polyamide (PA), displayed improved thermal and mechanical properties. The occurrence of transamidation reactions accompanied by the breakdown of the PTFE agglomerates resulted in the formation of a strong interphase between the components. In contrast, in the present system, the lack of thermal stabilization under air and the moderate thermal reinforcement observed under nitrogen atmosphere are probably indicative for the absence of chemical links between the PTFE cores and the PMMA of the shell. In these conditions only a physical shield can be exerted by the PTFE cores to the PMMA matrix.

To confirm that only a weak interface is present between the PTFE and the PMMA a preliminar dynamic-mechanical investigation was performed in the linear viscoelasticity region at the frequency of 1 Hz, between 40 °C and the temperature at which the samples lost their dimensional stability, with a heating rate of 4 °C/min. The samples for the dynamic-mechanical analysis were prepared simply by hot pressing the powder polymer sample into a rectangular mould at 160 °C for 20 min. No structural ordering was attempted. Figure 7 illustrates collectively the trends of the storage modulus E' and tan δ, for the three samples as a function of the temperature. The dynamic storage modulus E', decreases with increasing temperature with a drop at about 165 °C, corresponding to the glass transition of the PMMA component. Below the glass transition temperature, the PMMA plateau modulus increases as the PTFE amount increases. A parallel decrease in the dumping is observed, as expected for composites based on rigid fillers. However, the temperature of the glass transition of the PMMA component is not affected by the PTFE amount and only a small broadening of the relaxation process in the high temperature side of the transition occurs thus further indicating negligible interfacial effects between the PMMA and PTFE components.

Conclusion

The present paper describes the thermal and dynamic-mechanical properties of three PTFE/PMMA nanoparticle samples. The thermal stability was investigated by thermogravimetric analysis. From a qualitative point of view, the thermal degradation features of the PMMA component is similar to the well known behavior of the radically polymerized PMMA. However, once isolated from the PTFE cores, the shell forming PMMA exhibits a lower thermal stability than the corresponding PMMA component in the presence of the PTFE. This phenomenon, which occurs under both thermal and oxidative degradation conditions, indicates a definite, though moderate, thermal reinforcement due to the morphology of the nanocomposites.

As the PTFE amount in the nanocomposite increases, an increase in the thermal stability was observed under nitrogen atmosphere but not under air. These observations suggest that only a physical shield could be exerted by the PTFE cores to the PMMA matrix due to a weak interface between the two components. DMA analysis confirms negligible interfacial effects between the PMMA and PTFE.

[1] E. Giani, K. Sparnacci, M. Laus, G. Palamone, V. Kapeliouchko, V. Arcella, *Macromolecules* **2003**, *36*, 4360.
[2] K. Sparnacci, D. Antonioli, S. Deregibus, M. Laus, T. Poggio, V. Kapeliouchko, G. Palamone, G. Zuccheri, R. Passeri, *Macromolecules* **2009**, *42*, 3518.
[3] V. Kapeliouchko, G. Palamone, T. Poggio, G. Zuccheri, R. Passeri, K. Sparnacci, D. Antonioli, S. Deregibus, M. Laus, *J. Polym Sci. Pol. Chem.* **2009**, *47*, 2928.
[4] M. Laus, K. Sparnacci, D. Antonioli, S. Deregibus, V. Kapeliouchko, G. Palamone, T. Poggio, G. Zuccheri, R. Passeri, *J. Polym Sci. Pol. Phys.* **2010**, *48*, 548.
[5] T. Kashiwagi, A. Inaba, J. E. Brown, K. Hatada, T. Kitayama, E. Masuda, *Macromolecules* **1986**, *19*, 2160.
[6] G. A. Wang, C. C. Wang, C. Y. Chen, *Polym. Degr. Stab.* **2006**, *91*, 2443.
[7] Y. H. Hu, C. Y. Chen, C. C. Wang, *Polym. Degr. Stab.* **2004**, *84*, 545.
[8] P. Meneghetti, S. Qutubuddin, *Thermochimica Acta* **2006**, *442*, 74.
[9] G. Pompe, L. Häußler, P. Pötschke, D. Voigt, A. Janke, U. Geißler, B. Hupfer, G. Reinhardt, D. Lehmann, *J. Appl. Polym. Sci.* **2005**, *98*, 1308.
[10] G. Pompe, L. Häußler, P. Pötschke, D. Voigt, A. Janke, U. Geißler, B. Hupfer, G. Reinhardt, D. Lehmann, *J. Appl. Polym. Sci.* **2005**, *98*, 1317.

